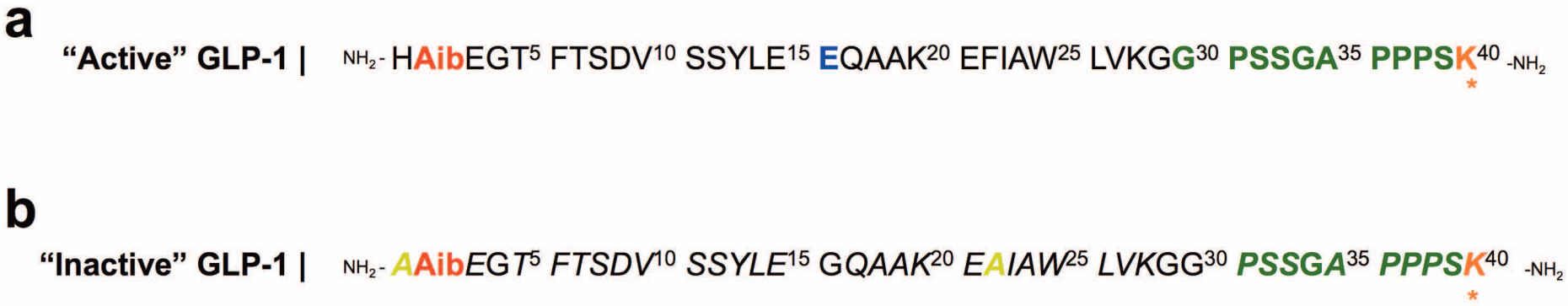
a
"Active" GLP-1 | NH2- HAibEGT5 FTSDV10 SSYLE15 EQAAK20 EFIAW25 LVKGG30 PSSGA35 PPPSK40 -NH2
*
b
"Inactive" GLP-1 | NH2- AAibEGT5 FTSDV10 SSYLE15 GQAAK20 EAIAW25 LVKGG30 PSSGA35 PPPSK40 -NH2
*

**Supplementary Table 1** ***In vitro*** **estrogen receptor and GLP-1 receptor activation/binding profiles**

| | | Estrogen Receptor α | | | | GLP-1 Receptor | | | |
|---|---|---|---|---|---|---|---|---|---|
| | Compound | $EC_{50}$ (nM) | s.d. | $IC_{50}$ (nM) | s.d. | $EC_{50}$ (nM) | s.d. | $IC_{50}$ (nM) | s.d. |
| Series 1 | GLP-1 | – | – | – | – | 0.011 | 0.002 | 0.381 | 0.043 |
| | GLP-1 analogue | – | – | – | – | 0.010 | 0.001 | 0.570 | 0.081 |
| | Stable GLP-1/estrogen | 108.2 | 15.73 | 1200 | 301.1 | 0.012 | 0.003 | 0.717 | 0.135 |
| | Stable GLP-1/estrogen | 0.013 | 0.001 | 198.0 | 16.75 | 0.014 | 0.001 | 0.627 | 0.046 |
| | 17 β-estradiol | 0.004 | 0.001 | 12.01 | 1.832 | – | – | – | – |
| | Estrone | 0.008 | 0.001 | 17.03 | 3.300 | – | – | – | – |
| | β-estradiol 3-acetyl-lysine amidomethyl ether | 0.563 | 0.027 | 235.0 | 28.81 | – | – | – | – |
| | β-estradiol 3-carboxymethyl ether | 0.033 | 0.018 | 130.4 | 19.95 | – | – | – | – |
| Series 2 | GLP-1/meta-stable estrogen 1 (hydrazone) | 1.181 | 0.165 | – | – | 0.011 | 0.002 | – | – |
| | GLP-1/meta-stable estrogen 2 (disulfide) | 265.3 | 13.95 | – | – | 0.010 | 0.001 | – | – |
| Series 3 | D-amino acid inactive GLP-1 analogue | – | – | – | – | 480.5 | 12.8 | – | – |
| | Inactive GLP-1/labile estrogen | – | – | – | – | 418.3 | 16.8 | – | – |
| | Inactive GLP-1/stable estrogen | – | – | – | – | 562.2 | 26.9 | – | – |

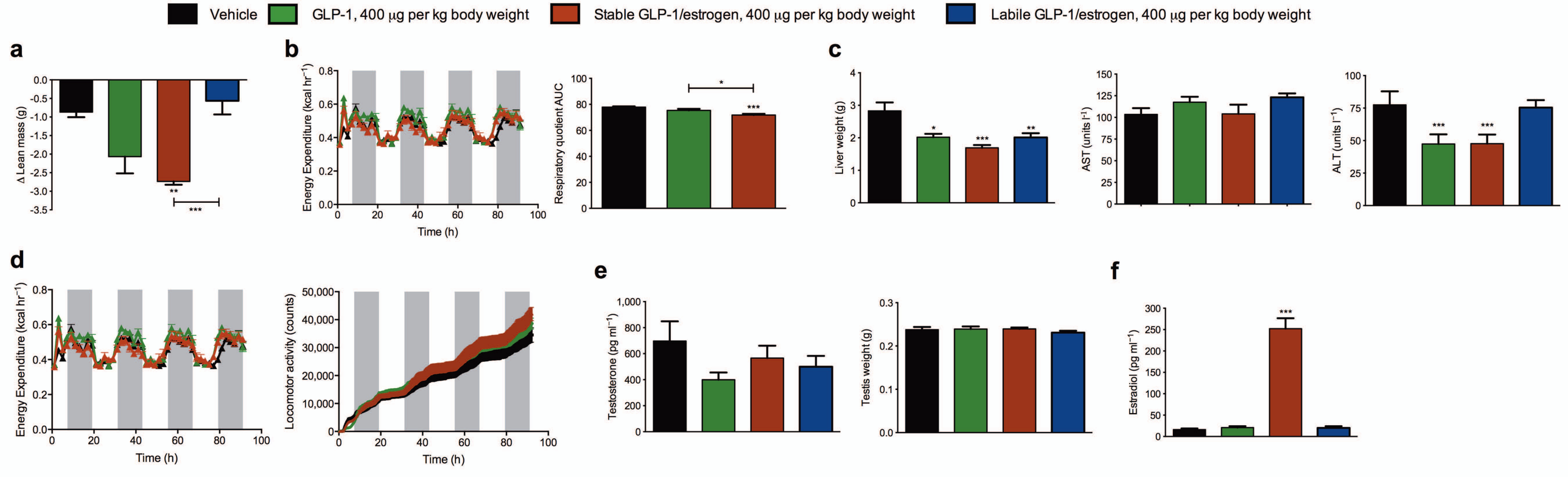
Vehicle
GLP-1, 400 μg per kg body weight
Stable GLP-1/estrogen, 400 μg per kg body weight
Labile GLP-1/estrogen, 400 μg per kg body weight
a
Δ Lean mass (g)
b
Energy Expenditure (kcal hr−1)
Time (h)
Respiratory quotient AUC
c
Liver weight (g)
AST (units l−1)
ALT (units l−1)
d
Energy Expenditure (kcal hr−1)
Time (h)
Locomotor activity (counts)
Time (h)
e
Testosterone (pg ml−1)
Testis weight (g)
f
Estradiol (pg ml−1)

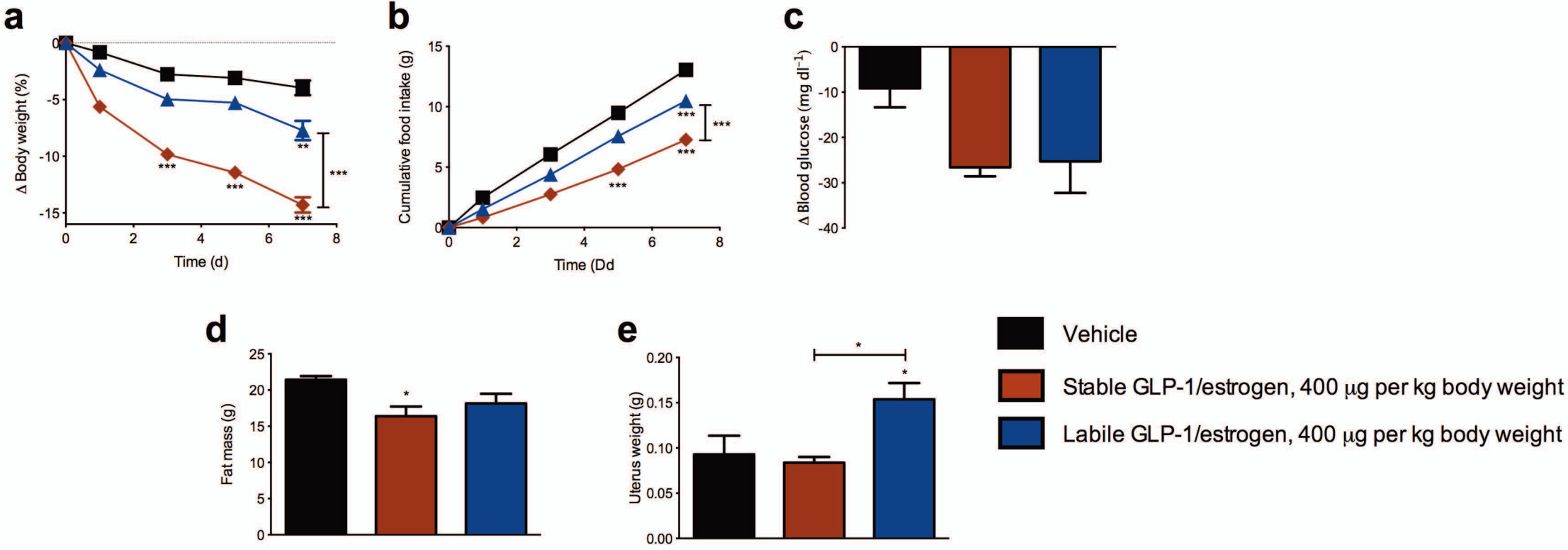
a
Δ Body weight (%)
Time (d)
b
Cumulative food intake (g)
Time (Dd
c
Δ Blood glucose (mg dl−1)
d
Fat mass (g)
e
Uterus weight (g)
Vehicle
Stable GLP-1/estrogen, 400 μg per kg body weight
Labile GLP-1/estrogen, 400 μg per kg body weight

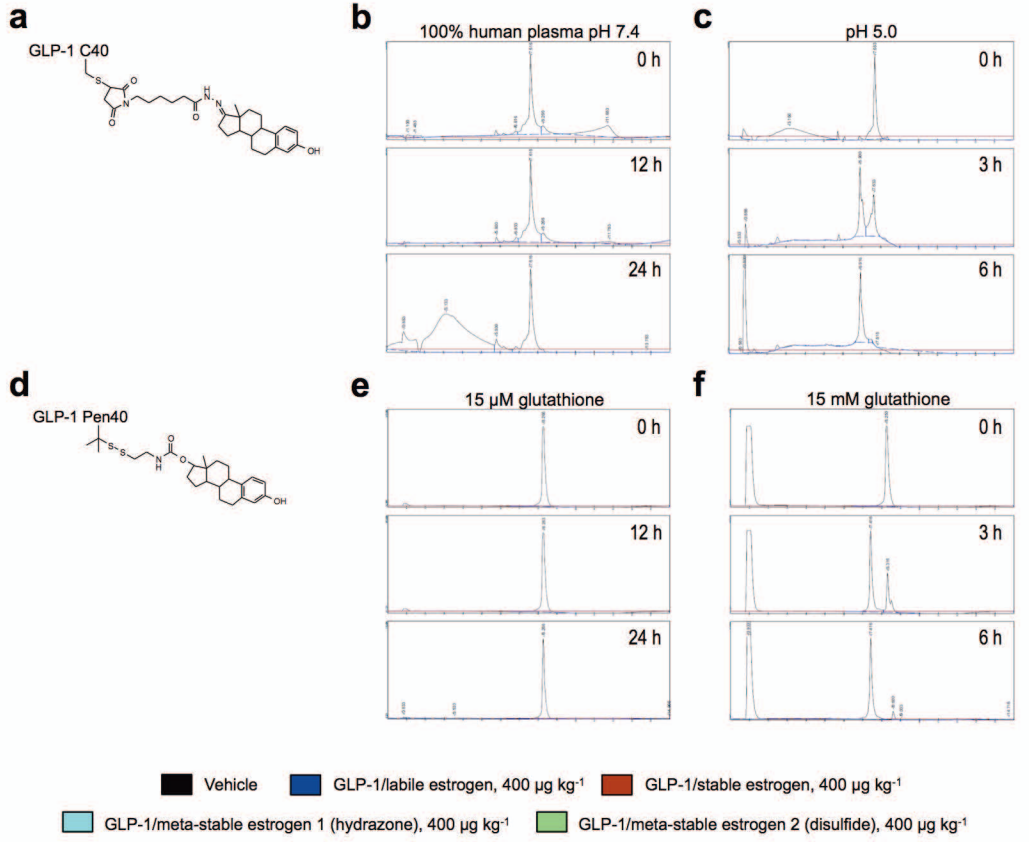
a
GLP-1 C40
b
100% human plasma pH 7.4
0 h
12 h
24 h
c
pH 5.0
0 h
3 h
6 h
d
GLP-1 Pen40
e
15 µM glutathione
0 h
12 h
24 h
f
15 mM glutathione
0 h
3 h
6 h
Vehicle
GLP-1/labile estrogen, 400 µg kg-1
GLP-1/stable estrogen, 400 µg kg-1
GLP-1/meta-stable estrogen 1 (hydrazone), 400 µg kg-1
GLP-1/meta-stable estrogen 2 (disulfide), 400 µg kg-1
g
Δ Body Weight (%)
Time (days)
***
h
Uterus Weight (g)
***
Day 7

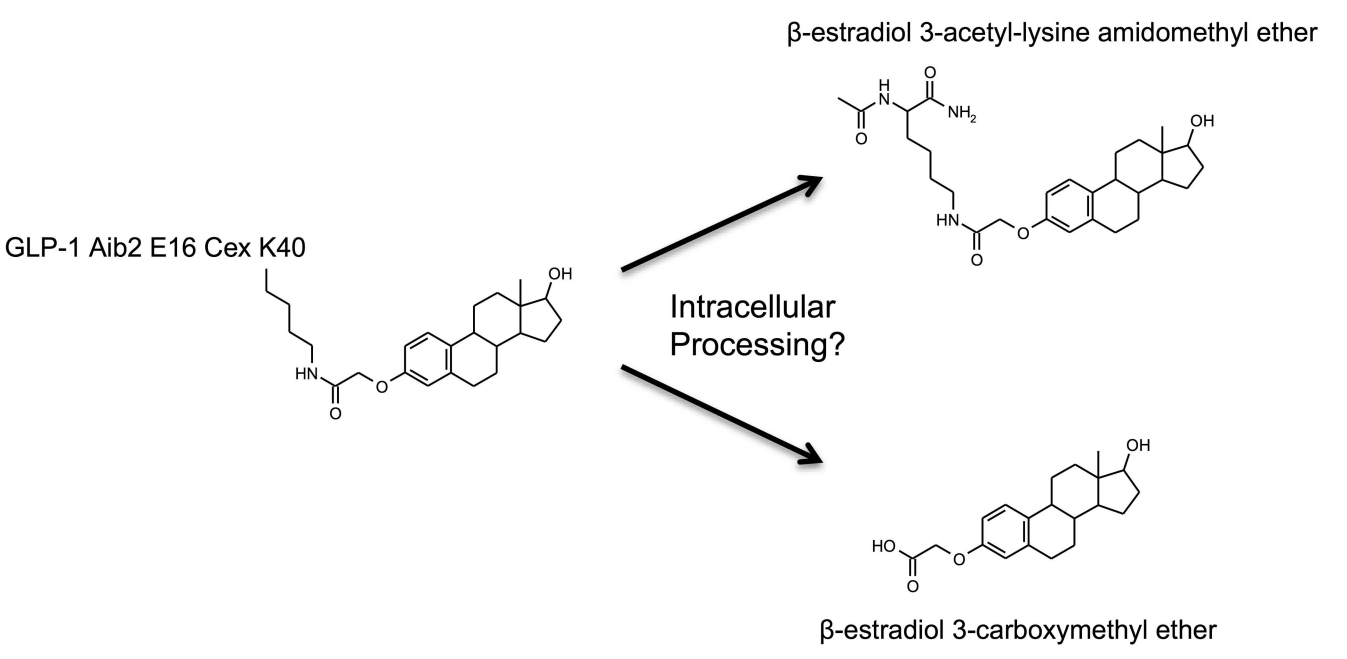
β-estradiol 3-acetyl-lysine amidomethyl ether
GLP-1 Aib2 E16 Cex K40
Intracellular
Processing?
β-estradiol 3-carboxymethyl ether

**Supplementary Table 2 *Ex vivo* whole body DXA measurements and pQCT measurements of femur**

DXA

| | | Mineral Content (mg) | | Area ($cm^2$) | | Mineral Density ($mg/cm^2$) | | Body Weight (g) | | Fat Mass (g) | | Lean Mass (g) | | % Conent in Relation to BW | |
|---|---|---|---|---|---|---|---|---|---|---|---|---|---|---|---|
| Treatment | Dose (mg/kg/day) | Mean | SEM | Mean | SEM | Mean | SEM | Mean | SEM | Mean | SEM | Mean | SEM | Mean | SEM |
| Vehicle | - | 786.00 | 28.80 | 13.13 | 0.28 | 59.73 | 1.10 | 43.41 | 1.15 | 30.12 | 0.54 | 9.62 | 0.38 | 1.81 | 0.06 |
| GLP-1 analogue | 400 | 761.00 | 20.80 | 13.16 | 0.21 | 57.81 | 1.99 | 38.19 | 0.65 | 27.27 | 0.76 | 8.76 | 0.21 | 1.99 | 0.04 |
| Labile GLP-1/estrogen | 400 | 743.00 | 26.20 | 12.84 | 0.27 | 57.80 | 1.31 | 37.21 | 1.06 | 26.16 | 1.03 | 9.46 | 0.27 | 2.00 | 0.03 |
| Stable GLP-1/estrogen | 400 | 662.00$^{*}$ | 24.60 | 12.07 | 0.30 | 54.79$^{**}$ | 0.74 | 32.76$^{***}$ | 0.98 | 21.60$^{***}$ | 0.80 | 9.08$^{ns}$ | 0.30 | 2.02$^{ns}$ | 0.03 |

pQCT

| | | Metaphysis Bone Content (mg) | | | | | | Diaphysis Bone Content (mg) | | | | | |
|---|---|---|---|---|---|---|---|---|---|---|---|---|---|
| | | Total | | Trabecular | | Cortical-Subcortical | | Total | | Trabecular | | Cortical-Subcortical | |
| Treatment | Dose (mg/kg/day) | Mean | SEM | Mean | SEM | Mean | SEM | Mean | SEM | Mean | SEM | Mean | SEM |
| Vehicle | - | 2.05 | 0.06 | 0.56 | 0.01 | 1.49 | 0.05 | 1.87 | 0.04 | 0.22 | 0.01 | 1.66 | 0.03 |
| GLP-1 analogue | 400 | 1.98 | 0.03 | 0.58 | 0.02 | 1.41 | 0.03 | 1.82 | 0.03 | 0.20 | 0.01 | 1.62 | 0.03 |
| Labile GLP-1/estrogen | 400 | 2.21 | 0.11 | 0.52 | 0.03 | 1.70$^{*}$ | 0.13 | 1.92 | 0.01 | 0.19 | 0.01 | 1.72$^{**}$ | 0.02 |
| Stable GLP-1/estrogen | 400 | 1.97 | 0.12 | 0.53 | 0.03 | 1.44 | 0.14 | 1.72 | 0.05 | 0.20 | 0.01 | 1.53 | 0.04 |

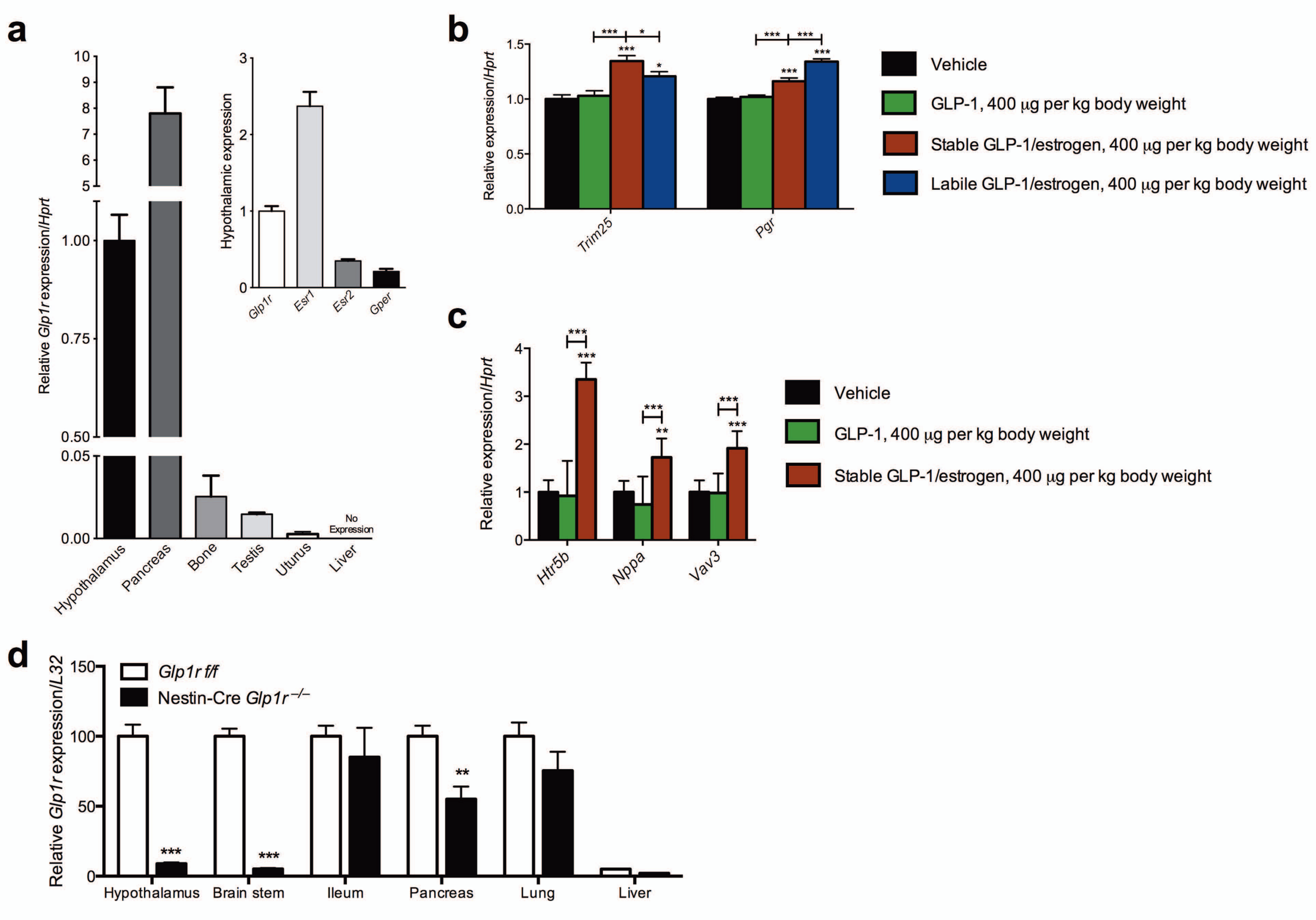
a
Relative Glp1r expression/Hprt
Hypothalamic expression
Glp1r
Esr1
Esr2
Gper
No Expression
Hypothalamus
Pancreas
Bone
Testis
Uturus
Liver
b
Relative expression/Hprt
Trim25
Pgr
Vehicle
GLP-1, 400 μg per kg body weight
Stable GLP-1/estrogen, 400 μg per kg body weight
Labile GLP-1/estrogen, 400 μg per kg body weight
c
Relative expression/Hprt
Htr5b
Nppa
Vav3
Vehicle
GLP-1, 400 μg per kg body weight
Stable GLP-1/estrogen, 400 μg per kg body weight
d
Relative Glp1r expression/L32
Glp1r f/f
Nestin-Cre Glp1r−/−
Hypothalamus
Brain stem
Ileum
Pancreas
Lung
Liver

**a**

GLP-1 Aib2 E16 Cex K40

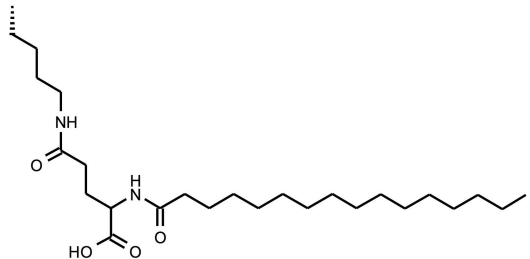


**b**

GLP-1 Aib2 E16 Cex K40

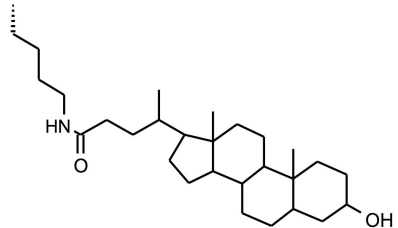

**Supplementary Figure 1.** Amino acid sequences of GLP-1 analogues. **(a)** Amino acid sequence of fully active GLP-1 analogue which features 2-aminoisobutyric acid at position 2 (red), glutamic acid at position 16 (blue), the C-terminal extension from exendin-4 from position 30-39 (green), and lysine-amide at position 40 (orange) with site of estrogen attachment (*). **(b)** Amino acid sequence of inactive GLP-1 analogue which is composed entirely D-amino acids (italicized) and features alanine at positions 1 and 22 (yellow), 2-aminoisobutyric acid at position 2 (red), the C-terminal extension from exendin-4 from position 30-39 (green), and lysine-amide at position 40 (orange) with site of estrogen attachment (*).

**Supplementary Table 1.** $EC_{50}$ values were generated from dose-response curves and represent compound concentrations at which half maximal activation occurred at either the estrogen receptor or GLP-1 receptor. $IC_{50}$ values were generated from dose-response curves and represent compound concentrations at which half maximal inhibition of competitor ligand occurred at either the estrogen receptor alpha or GLP-1 receptor. A minimum of three separate experiments was conducted for each compound at both estrogen and GLP-1 receptors.

**Supplementary Figure 2.** Two-week treatment of diet-induced obese male mice with GLP-1/estrogen conjugates. **(a)** Effects on lean mass ($n$ = 8) following daily subcutaneous injections of a GLP-1 analogue (green), a stable GLP-1/estrogen conjugate (red) and a labile GLP-1/estrogen conjugate (blue) at a single dose of 400 μg $kg^{-1}$. In separate experiments, **(b)** respiratory quotient, **(c)** liver weights and plasma AST/ALT, **(d)** energy expenditure and locomotor activity, **(e)** plasma testosterone and testes weight and **(f)** plasma estradiol were monitored throughout 2-weeks of treatment with the GLP-1 analogue, stable conjugate and labile conjugate at the equivalent dose of 400 μg $kg^{-1}$ ($n$ = 8). Data in **a-f** represent means ± s.e.m. *$P$ < 0.05, ** $P$ < 0.01, *** $P$ < 0.001, determined by analysis of variance (ANOVA) comparing vehicle to compound injections unless otherwise noted.

**Supplementary Figure 3.** One-week treatment of diet-induced obese female ovariectomized mice with GLP-1/estrogen conjugates. **(a)** Effects on body weight, **(b)** cumulative food intake, (**c)** *ad lib* blood glucose, **(d)** fat mass, and **(e)** uterus weight ($n$ = 8) following daily subcutaneous injections of a labile GLP-1/estrogen conjugate (blue) and stable GLP-1/estrogen conjugate (red) at a single dose of 400 μg $kg^{-1}$. Data in **a-e** represent means ± s.e.m. *$P$ < 0.05, ** $P$ < 0.01, *** $P$ < 0.001, determined by analysis of variance (ANOVA) comparing vehicle to compound injections unless otherwise noted.

**Supplementary Figure 4.** Structure, stability profiles and *in vivo* metabolic activity of meta-stable GLP-1/estrogen conjugates. **(a)** Structure of the GLP-1/meta-stable estrogen conjugate #1 featuring a hydrazone bond linkage to

estrogen. HPLC traces of sequential time point aliquots of the hydrazone-based meta-stable conjugate throughout incubation at 37°C in **(b)** 100% human plasma at pH 7.4 and **(c)** pH 5.0 buffer. **(d)** Structure of the GLP-1/meta-stable estrogen conjugate #2 featuring a hindered disulfide bond linkage to estrogen. HPLC traces of sequential time point aliquots of the hydrazone-based meta-stable conjugate throughout incubation at 37°C in buffer containing **(e)** 15 μM glutathione (mimics extracellular thiol concentrations) and **(f)** 15 mM glutathione (mimics extracellular thiol concentrations). **(g)** Effects on body weight in DIO mice ($n$ = 8) and **(h)** uterus weight in OVX mice ($n$ = 8) following daily subcutaneous injections of a labile conjugate (dark blue), stable conjugate (dark red), acid-sensitive hydrazone-based meta-stable conjugate (cyan), and reduction-sensitive disulfide-based meta-stable conjugate (neon green) at a dose of 400 μg $kg^{-1}$. Data represent means ± s.e.m. *** $P < 0.001$, determined by analysis of variance (ANOVA) comparing vehicle to compound injections unless otherwise noted.

**Supplementary Figure 5.** Structures of potential intracellular estrogen metabolites liberated from the stable GLP-1/estrogen conjugate. Calculated $EC_{50}$ values are shown in **Supplementary Table 1**.

**Supplementary Table 2.** Whole body DXA measurements (excluding the head) of bone mineral content, bone area, bone mineral density, fat mass, and lean mass as well as femoral metaphysis and diaphysis bone contents (total, trabecular, and cortical-subcortical) as measured by *ex vivo* pQCT of DIO male mice treated for 14 days with the GLP-1 conjugates at a dose of 400 μg $kg^{-1}$. Data represent means ± s.e.m. *$P < 0.05$, ** $P < 0.01$, and *** $P < 0.001$, determined by analysis of variance (ANOVA) comparing vehicle to compound injections unless otherwise noted.

**Supplementary Figure 6.** GLP-1R gene expression profile and hypothalamic gene expression patterns from mice treated with GLP-1/estrogen conjugates. **(a)** Tissue expression profile of the GLP-1R gene in C57BL/6 mice with hypothalamic expression of GLP-1R and estrogen receptor genes in the insert. Effects on hypothalamic gene expression of *trim25* and *pgr* (progesterone receptor) in **(b)** ovariectomized female mice following acute treatment (3 days) or **(c)** male DIO mice treated chronically (14 days) with daily subcutaneous injections of a GLP-1 analogue (green), stable GLP-1/estrogen conjugate (red) or labile GLP-1/estrogen conjugate (blue) at a dose of 400 μg $kg^{-1}$. **(d)** Tissue expression profile of the GLP-1R gene in generated Nestin-Cre *Glp1r*$^{-/-}$ mice. Data **(a-d)** represent means ± s.e.m. *$P < 0.05$, ** $P < 0.01$, *** $P < 0.001$, determined by analysis of variance (ANOVA) comparing vehicle controls to compound injections unless otherwise noted.

**Supplementary Figure 7. (a)** Structure of GLP-1/γGlu-γGlu-palmitate conjugate. **(b)** Structure of GLP-1/lithocholic acid conjugate.